CHEMICAL ENGINEERING TRANSACTIONS
VOL. 55, 2016
A publication of AIDIC
The Italian Association of Chemical Engineering
Online at www.aidic.it/cet
Guest Editors:Tichun Wang, Hongyang Zhang, Lei Tian

ISBN978-88-95608-46-4; **ISSN** 2283-9216
DOI: 10.3303/CET1655034

Optimization Design of Friction Drum of Farm Winch

Chuanyu Wu[a]*, Chengjun Zhou[a], Xinnian Zhou[a], Zhengxiong Zhang[a], Rongfeng Shen[a], Huoming Zhang[b]

[a] Fujian Agricultural and Forestry University, China;
[b] Zhangping fifty-one State Forestry Center, China.
627467445@qq.com

The friction traction and radial composite stress of each ring of traditional friction roll have a huge difference. In order to solve the problem the paper has a conclusion through mechanical analysis and experimental verification, that the radial integrated stress of each ring is the same when the friction traction is same. Each groove of multi-groove friction roll is designed with different section according to the results of mechanical analysis, and then the different groove has different equivalent friction coefficient. As a friction reel with 2-slot, which equivalent friction coefficient of one groove is 0.6, another one is 0.2. Such 2-slot friction reel can provide the traction force as well as the traditional 4-slot friction do, so that the volume can be reduced by one half. The difference of each groove of 2-slot friction reel is less than 5%, which is less than 1% of the difference of traditional friction reel. So this friction reel with various section grooves is a good way of winch lightweight design for its force balance and light weight.

1. Introduction

Project ropeway is an efficient and environmental-friendly transportation system, which has found wide applications in the field of mineral products, forestry and so on (Cambi et al, 2015; Zhang et al, 2013; Cavalli, 2012). The recent decade has witnessed its application to agricultural planting, interfiling and harvest transportation (Zhang et al, 2012). However, agricultural materials are relatively lighter than mineral products and forestry. The planting ground is relatively small and scattered. Therefore, its traditional applications are restricted to large-scale winches in the mining and forestry industry. It is not suitable to the agricultural field, thus failing to achieve large-scale promotion (Zhang et al, 2013). Therefore, small scale and convenient transfer are deciding features of the agricultural ropeway.

A critical device influencing the miniaturization of the engineering ropeway is its driver, the winch. The twining coiling block of the traditional winch calls for certain rope capacity and a huge structure. Theoretically speaking, the friction coiling block is not limited by distance and rope capacity, and is simple in structure, light in weight. Therefore, to replace the twining coiling block with the friction coiling block is a valid approach to achieve lightweight design of the winch. [5] However, the friction coiling block relies on the friction between the steel wire rope and the friction coiling block to achieve traction (Krishnadev et al, 2010). Due to the restriction of the friction force, the traction is relatively small, which is only two thirds of the twining coiling block.

Traditionally, in order to increase the fraction (Figure 1), the number of coils is increased and the wrap angles are increased (Zhang and Xia, 2011). The friction force obtained by the steel wire rope of the traditional multi-coil block differs greatly, and the friction force from the rope exit end of the loose side to the rope entrance end of the tight side registers exponential increase. As a result, the friction traction obtained by the steel rope of the loose side is relatively smaller, which cannot make full use of the traction capability of various coils of the steel rope, and there is room for the optimization of the weight of the friction coiling block. (Wang et al, 2015) Therefore, how to strike a balance of the friction traction generated by various coils of the coiling block through optimized design of the friction coiling block structure is a key to realizing lightweight design of the winch (Ravindra et al, 2010) and constitutes the research significance of this paper.

Please cite this article as: Wu C.Y., Zhou C.J., Zhou X.N., Zhang Z.X., Shen R.F., Zhang H.M., 2016, Optimization design of friction drum of farm winch, Chemical Engineering Transactions, 55, 199-204 DOI:10.3303/CET1655034

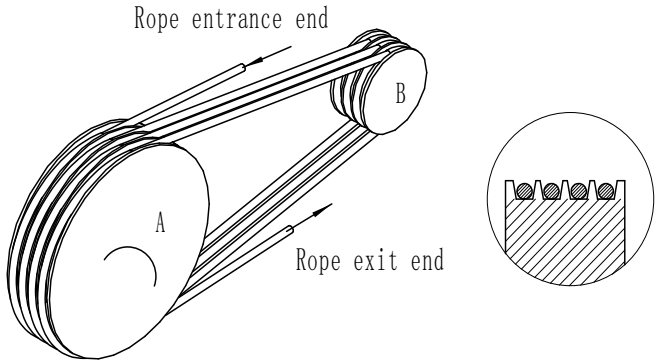

Figure 1: Multi-slot friction reel

2. Force analysis of the traditional friction coiling block

As is shown in Figure 2, the active friction coiling block, A, in the multi-groove coiling block is adopted as the analysis objective to analyse its force situation. The active friction coiling block contra rotates. The tensile force imposed on every groove on the section of the rope entrance end is expressed as:

$$T_i = T_i' e^{\mu a} \tag{1}$$

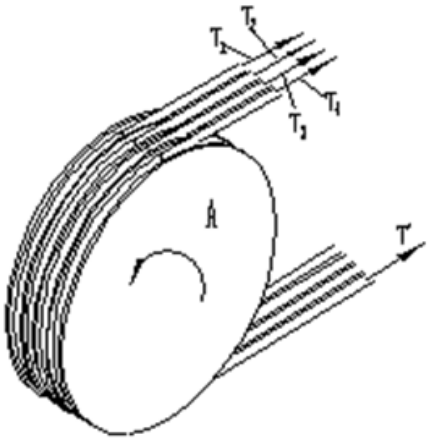

Figure 2: Force diagram of driving wheel

Where, Ti—stands for the tensile force of No. i groove on the loose side, (N);
Ti'— stands for the tensile force of No. i groove, (N);
μ—stands for the friction coefficient;
a— stands for the wrap angle, (radian)
Assuming that the tensile force of the loose side of the rope exit end is 10N; the friction coefficient is 0.2; the driven pulley is the ideal lubricating condition; and the tensile force of the back groove on the loose side is equal to that of the former groove on the tight side. Calculate the tensile force of every groove on the tight side. (See Table 1) From Table 1, it can be seen that the groove of traditional friction coiling blocks has the same structure and friction side conditions, but the friction traction thus generated differs greatly. The tensile force increases from the rope entrance end of the loose side to the rope exit end of the tight side in the friction coiling block. The tensile force of the fourth groove is about 6.55 times more than that of the first groove. The positive pressure imposed on the former also rises. Coiling block, A, of the dual-friction coiling block in Figure 1 still serves as an example. Adopt one tiny unit of the ring groove rope entrance end of A for mechanical (radial direction force) analysis. The tiny unit suffers the force from two directions. (Shown in Figure 3)

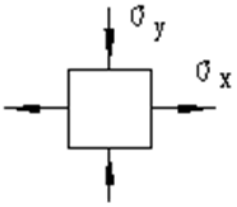

Figure 3: Stress analysis

$$\sigma_x = \frac{F}{aD} \tag{2}$$

$$\sigma_y = \frac{N}{aD} = \frac{F}{aD\mu} \tag{3}$$

Where, N—stands for the positive pressure, (N);
F—stands for the friction force, (N);
D—stands for the diameter of the coiling block, (mm);
Assume that F/aDis A. Put Eq. (2) and Eq. (3) into the fourth strength theoretical equation:

$$\sigma_s = \sqrt{\frac{1}{2}[(\sigma_y - \sigma_x)^2 + \sigma_y{}^2 + \sigma_x{}^2]} \tag{4}$$

$$\sigma_s = \sqrt{\frac{1}{2}\left[A^2 + (\frac{A}{\mu})^2 + (A - (\frac{A}{\mu})^2 \right]} = A\sqrt{1 + \frac{1}{\mu^2} - \frac{1}{\mu}} \tag{5}$$

Assume that D is “1.” Place the tensile force of Table 1 on the tight side into Eq. (5). Work out the stress, σ_s, and refer to Table 1 for results. From Table 1, it can be seen that the stress of various grooves differs greatly and that the stress of the fourth groove is 6.55 times higher than that of the first groove. In other words, the stress is in direct proportion to the friction fraction of various grooves, and features a huge difference.

Table 1: Tight side tension and stress of traditional grooves when loose side tension is 10 N

	Groove 1	Groove 2	Groove 3	Groove 4
Tensile force on the tight side(*T*), N	18.7	35.1	65.8	123.3
Compound stress at the radial direction (σ_s), kPa	12.8	23.9	44.7	83.9

3. Optimization design of the friction coiling block’ cariable cross section

According the force analysis of the former part, if friction traction of every groove of the friction coiling block gets near to each other and the stress of every groove is evenly distributed, its structural stress performance can be improved. At the same time, the structural strength of the whole friction coiling block can be fully utilized so as to effectively alleviate the weight and improve the service life.

To the end, the concave-groove of the friction coiling block is designed into the groove shape on different cross sections. (See Figure 4) The left groove is the traditional ring groove; while the right groove is designed into the concave-groove with the arc surface on two sides and being slotted at the bottom. By changing the slotting angle at the bottom of the ring slot, θ1, the concave-groove of the friction coiling block with different friction coefficients is obtained.

In order to simplify the calculation, it is assumed that the steel rope is rigid. Pressure Q is evenly distributed on the x coordinate, and the value of the positive pressure is:

$$N = \int_{\theta_0}^{\theta_1} \frac{\frac{Q}{2}}{(\cos\theta_0 - \cos\theta_1)} \times \frac{1}{\sin(\theta)} d\theta \tag{6}$$

Then:

$$N = \frac{Q}{2(\cos(\theta_0) - \cos(\theta_1))}(\ln(\tan(\frac{\theta_1}{2}) - \ln(\tan(\frac{\theta_0}{2}))) \quad (7)$$

At the same time, the friction force is:

$$F = 2\mu N = (\mu \frac{\ln(\tan(\frac{\theta_1}{2})) - \ln(\tan(\frac{\theta_0}{2}))}{(\cos(\theta_0) - \cos(\theta_1))})Q = \mu_v Q \quad (8)$$

Then,

$$\mu_v = \mu \frac{\ln(\tan(\frac{\theta_1}{2})) - \ln(\tan(\frac{\theta_0}{2}))}{(\cos(\theta_0) - \cos(\theta_1))} \quad (9)$$

Then,

$$F = T_0(e^{\mu_v a} - 1) \quad (10)$$

Where, Q—stands for the stress imposed on the radial direction of the roiling block on the steel rope, (N);
θ_0—stands for the starting angle of the arc, (°);
θ_1—stands for the end angle of the arc, (°).
According to Eq. (9), the double-groove friction coiling block in Figure 4 is designed as below: Groove 1 is consistent with the traditional groove and the friction coefficient is 0.2; the slotting angle of Groove 2, θ_0, is 15° and θ_1 is the 40° compound section concave-groove with the equivalent friction coefficient of 0.6. Put the equivalent friction coefficient into Eq. (10) and Eq. (5) to work out the friction force and the stress. (See Table 2)

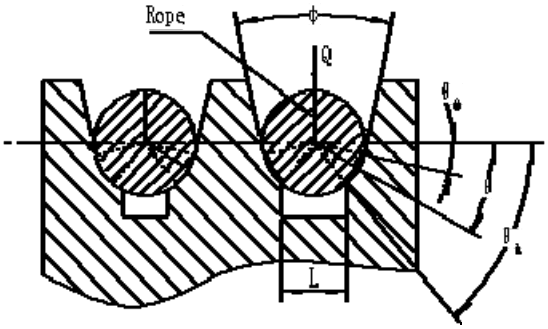

Figure 4: Cross section structural chart of the variable cross-section friction coiling block

Table 2: Tight side tension and stress of variable cross-section grooves when side tension is 10 N

	Groove 1	Groove 2
Tensile force on the tight side (*T*), N	65.8	123.3
Compound stress on the radial direction (σ_s), kPa	81.43	83.9

From the data in Table 1 and Table 2, it is obvious that, when the tensile force of the traditional multi-groove friction coiling block on the loose side is 10N, the tensile force passing the friction coiling block of Groove 4 on the tight side is 123.3N. The tensile force and the stress of every groove undergo great changes. The stress on every groove of the whole friction coiling block is seriously uneven.
The variable cross-section multi-groove friction coiling block after optimized design is a dual-groove friction coiling block. From Table 2, it can be seen that the tensile force imposed on the traditional multi-groove friction coiling block on the loose side is 10N. After undergoing the friction traction of dual-groove variable cross-

section friction coiling block, the figure can increase to 123.3N. Besides, the stress of Groove 1 and Groove 2 is close to each other, registering a difference of less than 5%. The force status has been obviously improved, and the volume of the friction coiling block can be reduced by 50%.

4. Confirmatory experiment

In order to verify the accuracy of theoretical analysis, model verification test is conducted of the variable cross-section concave-groove friction roiling block. The test model is shown in Figure 5, which is made up of the coiling block, the steel rope, the weight on the loose side and the tension meter. The coiling block model is a cylinder with a diameter of 40mm. On its surface, there is a 40° compound ring groove 1 with the cross section wedge angle of θ1 and a flat base ring groove 2 (wedge angle, θ1=180°). The test load adopts the weight. The traction is measured by the Aidebao HP-1K tension meter. The tensile force on the tight side obtained is shown in Figure 3. The value of the corresponding friction force and the stress is calculated respectively. (See Table 3)

From the data in Table 3, it can be seen that different slotting angle will lead to different friction coefficients, and that different friction coefficients and tensile force on the tight side can be obtained. According to Eq. (5), the stress of every groove worked out is almost the same so as to achieve a balanced distribution of the stress of every groove of the friction coiling block. Therefore, the friction coiling block can be designed into multiple ring-groove friction coiling block with different sections and equivalent friction coefficients on every ring groove. Through proper increase of the equivalent friction coefficient on the rope exit direction on the loose side, and its contact positive pressure and friction force, the stress distribution on every groove of the friction coiling block can be balanced, the number of the coiling block's ring-grooves and the weight of the friction roiling block can be reduced.

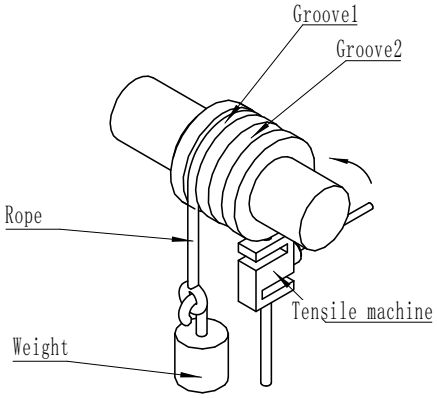

Figure 5: Test model

Table 3: Verification test data table

Wedge angle of the cross section θ_1, °	Tensile force on the loose side, N	Equivalent friction coefficient	Tensile force on the tight side, N	Friction force, N	Computed stress, kPa
40	4	0.59	25.7	21.7	0.785
180 (Flat base)	25	0.20	47	22	0.797

5. Conclusions

The structure of various concave-grooves of the traditional friction coiling block is similar to each other. Due to the friction caused by coiling, it can be seen from the force analysis that the friction force registers exponential increase from the rope exit end on the loose end to the rope entrance end on the tight end, thus resulting in huge changes of stress distribution of the friction coiling block along the axial direction, and inadequate utilization of the structural strength of the friction coiling block. Concerning the problem, the traditional friction coiling block is optimized into a variable cross-section concave-groove friction coiling block. Through the variation of the concave-groove cross-section shape and slotting angle, the equivalent friction coefficient and

friction of the concave-groove of the rope exit end on the loose side can be improved, thus ensuring the stress of various grooves to stay close to each other. The calculation and analysis results suggest that the stress of various cross-section multiple ring grooves reaches a balance. The maximum difference of stress among various grooves is just 0.03 times or 3.03%. However, the maximum difference of stress among various grooves of Groove 4 traditional friction coiling block is 5.55 times or 555.46%. At the same time, the traction capability of the multiple concave-groove friction coiling blocks is significantly increased. The traction of the dual concave-ring variable cross-section friction coiling block can reach the traction of Groove 4 traditional friction coiling block, and its weight can be reduced by 50%. Therefore, the dual-groove variable cross-section friction coiling block can not only improve the overall friction traction, but also the axial stress characteristics and force property of the friction coiling block. Besides, the volume can be reduced by 50%. All these research findings are of high referential value to the lightweight design of winches.

Acknowledgments

This work was supported by The National Natural Science Foundation of China (General Program, 30972359), Fujian Provincial Forestry Department projects (Fujian Forestry[2014]2), Zhangping fifty one State Forestry Center cooperation project funds (KH1400850), Fujian Agriculture and Forestry University class universities funded projects (113-612014018)

Reference

Cambi M., Certini G., Neri F., Marchia E., 2015, The impact of heavy traffic on forest soils: a review, Forest Ecology and Management, 338, 124-138, DOI:10.1016/j.foreco.2014.11.022.

Cavalli R., 2012, Prospects of Research on Cable Logging in Forest Engineering Community, Croatian Journal of Forest Engineering, 33, 339-356.

Krishnadev M., Larouche M., Lakshmanan V.I., Sridhar R., 2010, Failure analysis of failed wire rope, Journal of Failure Analysis and Prevention, 10, 341-348. DOI: 10.1007/s11668-010-9367-2.

Ravindra V., Padmanabham C., Sujatha C, Sujatha C., 2010, Static and free vibration studies on a pulley-belt system with ground stiffness, Journal of the Brazilian Society of Mechanical an Engineering, 32, 61~70, DOI: 10.1590/S1678-58782010000100009.

Wang X.C., Wang L., Shen B., Sun F.H., 2015, Friction and wear performance of boron doped, undoped microcrystalline and fine grained composite diamond films, Chinese Journal of Mechanical Engineering, 28, 155-163, DOI: 10.3901/CJME.2014.1114.168.

Zhang C.P., Wang Q.Y., Zhang P., Yu P., Lin W., 2013, Analysis and Research of the Winch System, Applied Mechanics and Materials, 401-403, 36-40.

Zhang C.P., Wang Q.Y., Zhang P., Yu P., Lin W., 2013, Analysis and Research of the Winch System, Applied Mechanics and Materials, 401-403, 36-40.

Zhang P.J., Pan M.X., Wang L.H., 2012, Optimal Design of Small Winching Drum Installed in Skidding Tractor Based on Computer Aided Design, Advanced Materials Research, 487, 277-280.

Zhang S.R., Xia X.H., 2011, Modeling and energy efficiency optimization of belt conveyors, Applied Energy, 88, 3061-3071, DOI:10.1016/j.apenergy.2011.03.015.